Science of the Total Environment 407 (2009) 3372–3384

Contents lists available at ScienceDirect

Science of the Total Environment

journal homepage: www.elsevier.com/locate/scitotenv

Mineralogical and geochemical controls of arsenic speciation and mobility under different redox conditions in soil, sediment and water at the Mokrsko-West gold deposit, Czech Republic

Petr Drahota [a,b,*], Jan Rohovec [b], Michal Filippi [b], Martin Mihaljevič [a], Petr Rychlovský [c], Václav Červený [c], Zdeněk Pertold [a]

[a] Institute of Geochemistry, Mineralogy and Mineral Resources, Faculty of Science, Charles University, Albertov 6, Prague 2, 128 43, Czech Republic
[b] Geological Institute, Academy of Sciences of the Czech Republic, v.v.i., Rozvojová 269, Prague 6 - Suchdol, 165 00, Czech Republic
[c] Department of Analytical Chemistry, Faculty of Science, Charles University, Hlavova 2030/8, Prague 2, 128 43, Czech Republic

ARTICLE INFO

Article history:
Received 29 July 2008
Received in revised form 7 January 2009
Accepted 12 January 2009
Available online 12 February 2009

Keywords:
Arsenic
Speciation
Soil and sediment
Mobility
(Bio)geochemical model

ABSTRACT

Naturally contaminated soil, sediment and water at the Mokrsko-West gold deposit, Central Bohemia, have been studied in order to determine the processes that lead to release of As into water and to control its speciation under various redox conditions. In soils, As is bonded mainly to secondary arseniosiderite, pharmacosiderite and Fe oxyhydroxides and, rarely, to scorodite; in sediments, As is bonded mainly to Fe oxyhydroxides and rarely to arsenate minerals.

The highest concentrations of dissolved As were found in groundwater (up to 1141 μg L^{-1}), which mostly represented a redox transition zone where neither sulphide minerals nor Fe oxyhydroxide are stable. The main processes releasing dissolved As in this zone are attributed to the reductive dissolution of Fe oxyhydroxides and arsenate minerals, resulting in a substantial decrease in their amounts below the groundwater level. Some shallow subsurface environments with high organic matter contents were characterized by reducing conditions that indicated a relatively high amount of $S^{-2,0}$ in the solid phase and a lower dissolved As concentration (70–80 μg L^{-1}) in the pore water. These findings are attributed to the formation of Fe(II) sulphides with the sorbed As. Under oxidizing conditions, surface waters were undersaturated with respect to arsenate minerals and this promoted the dissolution of secondary arsenates and increased the As concentrations in the water to characteristic values from 300 to 450 μg L^{-1} in the stream and fishpond waters. The levels of dissolved As(III) often predominate over As(V) levels, both in groundwaters and in surface waters. The As(III)/As(V) ratio is closely related to the DOC concentration and this could support the assumption of a key role of microbial processes in transformations of aqueous As species as well as in the mobility of As.

© 2009 Elsevier B.V. All rights reserved.

1. Introduction

In natural systems, As exists essentially in four oxidation states (−III, 0, +III, and +V), as both inorganic and organometallic species. Most of the naturally occurring As is contained in inorganic compounds (Cherry et al., 1979; Cullen and Reimer, 1989), where the relative proportions of As(V) and As(III) species are governed by three main environmental factors: the redox potential, the pH and the biological activity (Cullen and Reimer, 1989). From the standpoint of thermodynamics, the predominant forms of dissolved As under oxidizing conditions are As(V) species ($H_2AsO_4^-$, $HAsO_4^{2-}$ and AsO_4^{3-}), whereas As(III) species ($H_3AsO_3^0$ and $H_2AsO_3^-$) predominate in reducing environments (Cherry et al., 1979; Sadiq, 1997). However, several studies have shown that the As(III) concentrations exceed those of As (V) in the permanently oxidizing environment of surface waters and soils, suggesting nonequilibrium thermodynamic conditions due to the slow oxidation kinetics of As(III) (e.g., Cullen and Reimer, 1989 and references therein; Bowell et al., 1994; Sohrin et al., 1997; Macur et al., 2001; Macur et al., 2004). Consequently, the distribution of As species is of considerable environmental concern, since As(III) is the most toxic As species (Cullen and Reimer, 1989).

Under normal soil conditions, the solubility, mobility and bioavailability of As are mostly driven by adsorption–desorption processes involving Fe, Al, Mn oxyhydroxides, clay minerals, carbonates (under oxidizing conditions) and sulphide minerals (under reducing conditions) (Cullen and Reimer, 1989; Sadiq, 1997). Moreover, secondary arsenate minerals can control the solubility of As when the amount of As exceeds the capacity of the available surface ligand-bonding sites and the concentrations of dissolved arsenate and metal cations exceed

* Corresponding author. Institute of Geochemistry, Mineralogy and Mineral Resources, Faculty of Science, Charles University, Albertov 6, Prague 2, 128 43, Czech Republic. Tel.: +420 221 951 498; fax: +420 221 951 496.
E-mail address: drahota@natur.cuni.cz (P. Drahota).

0048-9697/$ – see front matter © 2009 Elsevier B.V. All rights reserved.
doi:10.1016/j.scitotenv.2009.01.009

the solubility product of the arsenate minerals. A series of secondary arsenate and sulphoarsenate minerals has been identified under oxidizing conditions, including soils, mine tailings and former industrial sites (Magalhães, 2002; Morin and Calas, 2006). Scorodite is the most common arsenate found in the weathering environment of As-bearing sulphide deposits (Dove and Rimstidt, 1985). Subsequent interactions with solutions may cause a shift in the pH to neutral values, with precipitation of Ca, Mg and K–Ba arsenates, such as arseniosiderite, haidingerite, hörnesite, pharmacolite, pharmacosiderite, picropharmacolite, weillite, etc. (Voight et al., 1996; Juillot et al., 1999; Morin et al., 2002; Filippi et al., 2004; Frau and Ardau, 2004; Paktunc et al., 2004). These arsenate minerals are metastable under most natural conditions and their persistence in nature suggests that their solubility may control the concentration of As in waters. This finding is also in accordance with the sparce solubility data available for arsenate minerals (Langmuir et al., 2006).

The goal of the present study is to describe the mineralogical and geochemical processes controlling the release and/or sequestration of As in various redox environments above the Mokrsko-West gold deposit. To achieve this goal, we investigated the As distribution in naturally contaminated soil, stream and fishpond sediments and waters under various redox conditions. We combined detailed mineralogical investigations of solid samples with geochemical observations and with chemical analyses of surface water, porewater and groundwater.

2. Geological and environmental background

The Mokrsko-West deposit (MWD) is unique among European Variscan gold deposits, both from the economic (gold reserves of about 100 t), and mining (unaffected by mining activities) points of view. The MWD is located in Central Bohemia, approximately 50 km south of Prague. Gold-bearing quartz veins and sheeted veinlets are the main types of mineralization in the deposit, which developed in the marginal part of the Variscan granodiorite belonging to the Central Bohemian pluton (Morávek et al., 1989).

The MWD is characterized by a low sulphide content (generally below 3 vol.%), quartz-dominated gangue with minor calcite and silicate minerals (plagioclase, titanite and sparse amphibole, chlorite, biotite) and by a lack of extensive hydrothermal alteration. Arsenopyrite (FeAsS) is the predominant sulphide (Morávek et al., 1989) and its weathering flux corresponds to approximately 95% of the total input of As into the soil (Drahota et al., 2006). Arsenic also occurs rarely in löllingite ($FeAs_2$), ullmannite (Ni(Sb,As)S) and as a trace element in pyrite (below 1 wt.%) (Malec, 1990). During weathering, the minerals are oxidized and this produces a series of secondary arsenates and As-bearing oxyhydroxides in the soil, namely, arseniosiderite [$Ca_2Fe_3(AsO_4)_3O_2 \cdot 3H_2O$], ferrihydrite [$5(Fe_2O_3) \cdot 9H_2O$], goethite [FeO(OH)], minerals of the pharmacosiderite series [K,Ba, Ca)$(Fe,Al)_4(AsO_4)_3(OH)_{4-5} \cdot 5\text{-}7H_2O$], and scorodite [$FeAsO_4 \cdot 2H_2O$] (Filippi et al., 2004; Drahota and Pertold, 2005; Filippi et al., 2007). The large extent of natural As contamination around the MWD is indicated by As levels in the soil of >200 mg kg^{-1} over approximately 1.12 km^2 (Janatka and Morávek, 1990).

The elevated As concentration in the ore and the mobility of As also constitute a potential environmental hazard with groundwater leaching from saprolite and soils. High concentrations of As in the groundwater (255–1690 μg L^{-1}) and surface water (50–340 μg L^{-1}) were encountered in shallow wells and a stream (Fig. 1), respectively (Jílek, 1985; Drahota and Pertold, 2005). The highest As concentrations were detected in the private wells of the village of Mokrsko which were used to supply drinking water until the symptoms of As-related peripheral vascular diseases were detected (Jílek, 1985).

The soils in the area can be defined as cambisols and gley soil and their thickness is between 1 and 10 m, depending on the topography and drainage (Morávek, 1991). The annual precipitation over the past 40 years averaged at 555 mm y^{-1}, and the average temperatures in July rose to 17 °C, decreasing down to −3 °C in January. Additional geological and climatic information can be found in Drahota et al. (2006) and Filippi et al. (2007).

3. Methods and materials

3.1. Soil and sediment sampling and preparation

The three sampling profiles lie at an increasing distance from the primary ore mineralization in the east (characterized by soil profile M1) to the gaining stream in the west (characterized by soil profile M3); soil profile M2 characterizes the relatively flat area in the surroundings of the village of Mokrsko (Fig. 1). Down hole (non-rotation) hammer-drilling equipment (Kobra, USA) was used to reach the relatively consolidated saprolite in a depth from 133 to 351 cm. The 22 soil samples studied were classified as slightly acidic brown soil (Cambisol) (FAO, 1998). Clayey-silt horizons were only found in the M3 profile; they correspond to gley soil. The sediment samples (S1, S2, S4) of the stream and one sample of the fishpond bottom (S7) were collected manually at a depth of 5 cm using a stainless steel trowel. The solid samples were rapidly (within 2 min) placed in N_2-filled sterile air- and water-proof polyethylene bags, deaerated in the field for 5 min with a stream of N_2 and then cooled during transportation until they could be processed in the laboratory. The samples were divided into several subsamples within 5 h of collection in the field. Some of them were immediately used for determination of water-soluble As-species, pH and Eh measurements, some of them were dried, homogenised and sieved through a 2 mm sieve to determine the total concentrations of the elements, and the remaining subsamples were frozen for mineralogical investigation. Immediately prior to the mineralogical investigation, the subsamples were removed from the bags, placed on a plastic sheet and allowed to dry and oxidize at room temperature (20–25 °C). The soil and sediment samples were then gently ground with a wooden roller and sieved through 0.25 and 0.125 mm sieves. The XRD of several untreated soil samples revealed the predominant soil mineralogy as quartz, plagioclase, orthoclase, biotite, and amphibole. The clay fraction predominantly contained kaolinite, vermiculite, chlorite, and mixed layered illite–smectite.

3.1.1. Geochemical and mineralogical analysis

The temperature, pH_{H2O} and the redox potential (Eh) of the stream and fishpond sediments were measured directly in situ, using Schott–Geräte Handylab 2 pH meter. The soil pH_{H2O} and Eh were measured within 8 h of sample collection using a 1:2.5 (w/v) ratio of untreated, homogenised solid–water suspension after 1-hour agitation (Pansu and Gautheyrou, 2006). The redox potential values measured in the field and laboratory were referred to the standard hydrogen electrode (SHE). The concentrations of SiO_2, Al_2O_3, CaO, MgO, Na_2O, K_2O, P_2O_5, SO_3, $S^{-2,0}$, Mn, Fe, Ba and As in the <2 mm fraction of homogenised soils and sediments were measured using an X-ray fluorescence spectrometer (XRF, ARL 9400 XP^+) with the Uniquant™ 4 analysis program (UNIQUANT 4, 1999). XRF Uniquant is a semi-quantitative method and the associated errors were estimated to be ±0.2 wt.% for SiO_2, ±0.1 wt.% for other major constituent oxides and ±0.01 wt.% for minor elements.

In order to characterize As-bearing minerals in the soils and sediments, heavy-minerals were separated using bromoform diluted with 1,4-dioxane ($d = 2.81$ g cm^{-3}) in the 0.25–0.125 mm fraction of 15 samples representing both stream (S1, S2, S4) and fishpond (S7) sediments and the samples from the soil profiles. The soil samples ($n = 11$) were selected according to the pedological and geochemical variations (e.g., the total As concentration in the soil, redox potential) along the soil profiles to take into account possible variations in the mineralogy of the As-bearing phases. A rough quantitative estimate of As-bearing phases (including Fe oxyhydroxides) in the bulk sample was carried out by point counting of the grains from the heavy-

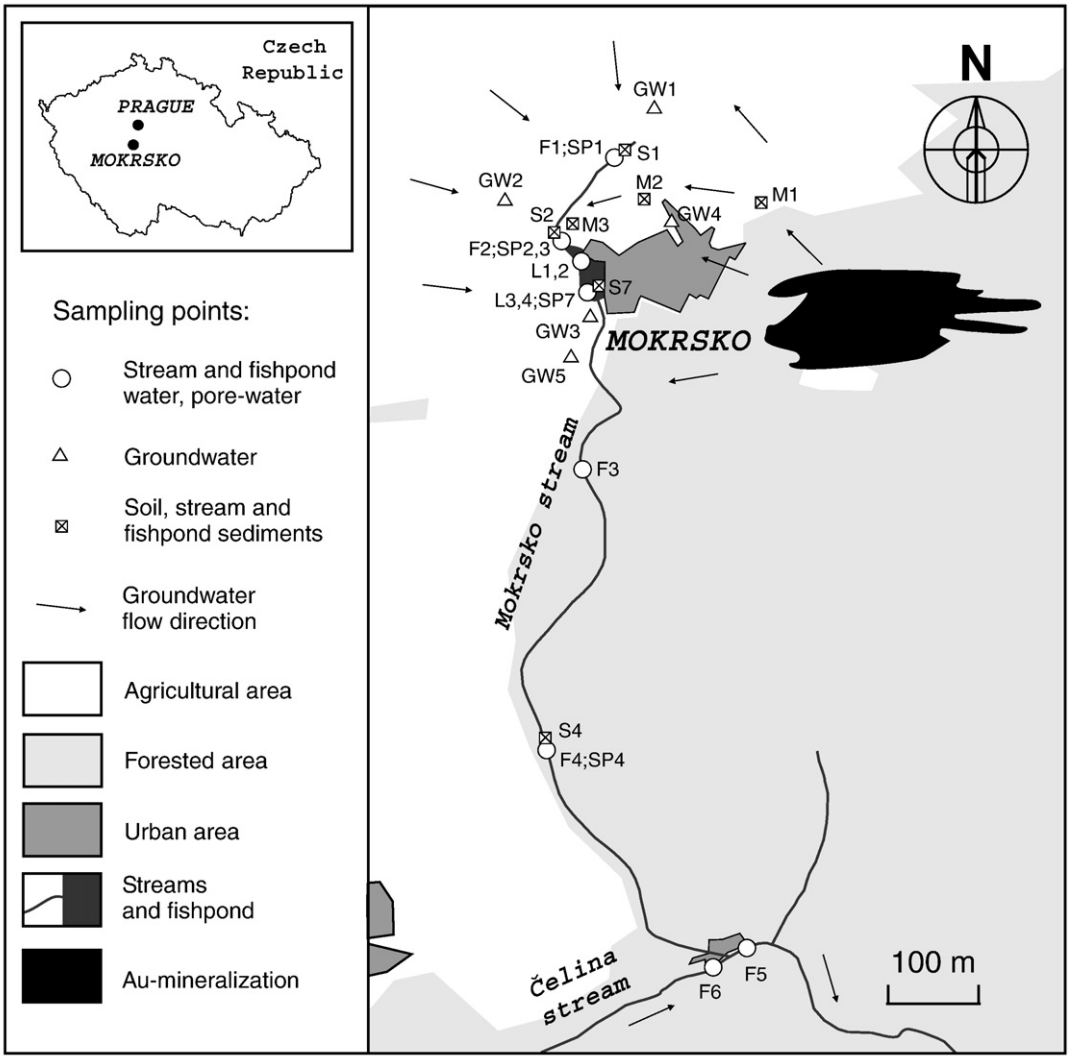

Fig. 1. Schematic map of the studied area with location of the sampling points. Waters: F—Mokrsko and Čelina streams, L—fishpond, GW—groundwater, SP—pore-water. Solids: M—soil profile, S—stream and fishpond sediments.

mineral 0.25–0.125 mm fraction. Heavy minerals were mounted on glass slides using polyester resin and thin sections were prepared. These polished thin sections of the heavy-mineral fraction were examined by scanning electron microscopy (SEM) and electron microprobe analysis (EMPA). The EMPA used a Cameca SX 100 microprobe equipped with four wavelength dispersion spectrometers (WDS), operating at 15 kV and 10 nA with 2 μm beam resolution and 10 s counting per element. Raw data were corrected for the atomic number, absorption and fluorescence effects (ZAF). The X-ray diffraction analyses (XRD) of the separated mineral phases from the pre-concentrated samples were performed using a PANalytical X`Pert Pro diffractometer equipped with a diffracted-beam monochromator and X`Celerator multichannel detector. The analysis conditions were as follows: CuKα radiation, 40 kV, 30 mA, step scanning at 0.02°/250 s in the range 3–70° 2θ. The qualitative analysis employed the X'Pert HighScore software 1.0d, equipped with the JCPDS PDF-2 database (ICDD, 2002).

3.1.2. Single extraction procedure

The water-soluble fraction of As(III), As(V) and some metals in 22 untreated soil samples was determined within 12 h after sample collection. Prior to the extraction procedure, the solutions were deaerated with a stream of N_2. Untreated and homogenised samples were subjected to ammonium oxalate extraction analysis in order to assess the degree of affinity of As for poorly crystalline Fe oxyhydroxides in soils and sediments.

The single extraction procedures were performed under the following conditions:

- Water-soluble As inorganic species: A 10 g sample were shaken at 20 rev. min^{-1} in 100 mL of deionised water (MilliQ+) for 1 h (adapted from Montperrus et al., 2002; Fernández et al., 2005).
- Oxalate-extractable As: A 2 g sample was shaken for 2 h in the dark at 20 rev. min^{-1} in 100 mL of 0.2 M ammonium oxalate adjusted to a pH of 3 with 0.2 M oxalic acid (e.g., Keon et al., 2001).

All the extractions were performed in acid-washed 100 mL HDPE centrifuge bottles. After shaking on a horizontal shaker, the solutions were centrifuged at 3000 rpm for 10 min. Decanted supernatants were treated and analysed by the same procedure as the water samples (see Section 3.2). A procedural blank was run for each extraction. The standard deviation for the second replicate of 5 randomly selected soil and sediment samples was lower than 10% of the individual values for a single extraction.

3.2. Water sampling and analysis

Water sampling was carried out on October 15 and 16 2005. Surface water samples were collected in duplicate from the Mokrsko

and Čelina streams at sites F1 to F6 and at the shallow fishpond (L1–L4) close to the village of Mokrsko (Fig. 1). In the fishpond, both the surface water (L1 and L3 samples) and the bottom water (L2 and L4 samples) were sampled. Groundwater samples were collected in duplicate from 5 selected well sites (GW1–GW5) close to the village of Mokrsko (Fig. 1). Groundwater was taken at shallow depths (0.5–6 m) by a battery-driven pump through a closed flow-through cell following stabilization of the pH, Eh, specific conductivity and turbidity (Puls and Paul, 1995). Flow rates did not exceed 500 mL min^{-1}. Porewater samples of saturated stream (SP1, SP2, SP3, and SP4) and fishpond sediments (SP7) were extracted by compression in the field (S1–S7). Waters were filtered in situ through 0.1 μm Millipore® membrane filters into HDPE bottles, and those destined for major cation and trace element analyses were adjusted to pH<2 with HNO_3 (Merck, Suprapur). Samples for the As redox species determination were filtered in situ through 0.1 μm filters into opaque 100 mL HDPE bottles, acidified to pH<2 with HCl (Merck, Suprapur), deaerated with N_2, and sealed in the field in N_2-filled gas-tight bags. Samples analysed for dissolved organic carbon (DOC) and anions were filtered through 0.45 μm cellulose nitrate membrane filters into glass vials and HDPE bottles, respectively, and left unpreserved. All the water samples were kept cool (4 °C) in an isothermal container during transportation and stored in a refrigerator until processing for the analysis. The temperature, pH, Eh and the specific conductivity were measured in the field, after their stabilization, with calibrated portable meters (Schott-Geräte Handylab 2), using a closed flow-through cell. The sensors were calibrated using a NIST-traceable calibration buffer (Hamilton Duracal). The accuracy of the pH, Eh, and specific conductivity measurements was ±0.01 std. pH unit, ±0.5 mV, and ±0.001 mS cm^{-1}, respectively. The field-measured redox potential values were referred to the SHE.

The total concentrations of dissolved As species (As(T) and As(III)) were measured using hydride generation atomic absorption spectrometry (HG-AAS) under the conditions described by Dedina and Tsalev (1995). The As(V) content was determined as the difference: $c_{As(V)} = c_{As(T)} - c_{As(III)}$. All the measurements were carried out on a SpectrAA 300 instrument (Varian, Australia) with deuterium background correction (As Super Lamp, Photron, Australia). The major cations were analysed by ICP-OES (IRIS Intrepid II XPS, USA). Quality control was performed by inserting a QC sample into the analytical run after each 10 samples. Field and laboratory duplicates indicate a relatively high level of reproducibility (<10%). Trace elements were determined by ICP-MS (VG Elemental PQ 3, UK). The measured concentrations of trace elements in the certified and synthetic standard (NIST 1640, 1643 d) were within ±5% of their certified values. Dissolved organic carbon (DOC) was analysed within 3 days on a Skalar Formacs^{HT} TOC/TN analyser. Anions (SO_4^{2-}, Cl^-, NO_3^-) were analysed by ion chromatography (HPLC, columns Tessek HEMA-S1000 Q-L 10 mm), F^- was determined potentiometrically using an ion-selective electrode (ISE); NH_4^+ was analysed spectrophotometrically using a Perkin-Elmer (Lambda 10, USA) analyser; the alkalinity was determined by titration (Metrohm, Switzerland) with 0.01 M H_2SO_4. The relative error of these analytical determinations was always <10%. The detection limits for the analysed elements are listed in Table 1.

3.3. Thermodynamic calculations

Version 6.2 of the PHREEQC geochemical code (Parkhurst and Appelo, 1999) with the included WATEQ4F database (Ball and Nordstrom, 1991) was used for the thermodynamic calculations in order (i) to speciate the waters and (ii) to determine the saturation indices (S.I.) of the waters in relation to the mineral phases. The WATEQ4F database was enlarged with data from the MINTEQ.V4 database for the solubility of ferrihydrite.

Table 1
The main physico-chemical characteristics of the water from the Mokrsko stream (F1–F4), the Čelina stream upstream (F6) and downstream (F5) from the confluence, the fishpond (L1–L4), the groundwater (GW1–GW5) and the pore water of sediment (SP1–SP7).

Sampling point	Field parameters				Major cations (mg L^{-1})					Major anions (mg L^{-1})						Minor and trace elements (mg L^{-1})																As species (mg L^{-1})			As(III)/As(V)	mg L^{-1} DOC
	pH	Eh	E.C.	T	Na	K	Ca	Mg	NH_4	HCO_3	SO_4	NO_3	Cl	PO_4	F	Fe	Mn	Al	Ba	Cd	Cu	Pb	Zn	Mo	Sb	As(III)	As(V)	As(tot)		
		mV	μS cm^{-1}	°C																																
DL									0.02	0.5	0.5	0.3	0.15	0.01	0.02	0.6	0.6	0.4	0.01	0.01	0.05	0.05	0.1	0.05	0.01	1		1.9		0.5
F1	7.65	462	622	7.9	14.3	4.25	85.6	18.8	0.07	109.8	141.9	66.9	40.9	0.06	0.22	18.1	173.5	<DL	53.17	0.03	0.66	0.06	1.7	1.34	2.13	47	402	449	0.1	2.5
F2	7.85	350	703	7.5	15.0	3.98	86.2	18.9	<DL	103.7	133.9	64.0	40.7	0.06	0.22	13.0	163.1	<DL	53.91	0.06	0.70	0.07	1.7	1.24	1.94	346	75	421	4.6	3.3
F3	7.62	363	590	6.0	15.9	4.94	75.5	16.3	<DL	152.6	87.7	23.4	35.6	0.23	0.24	16.5	29.2	<DL	70.23	0.02	0.73	0.09	16.5	1.29	0.87	297	13	310	22.9	4.5
F4	7.85	400	879	7.2	16.1	3.48	114.2	22.7	<DL	152.6	106.7	137.9	55.1	0.06	0.14	7.0	4.9	<DL	93.21	0.02	0.63	0.10	2.0	0.76	0.39	41	16	57	2.6	2.4
F5	8.23	395	700	5.6	19.6	6.66	82.8	18.3	<DL	143.4	110.7	41.7	48.3	0.28	0.13	34.0	18.2	<DL	63.21	0.02	1.01	0.11	32.5	1.31	0.35	2	30	32	0.1	4.2
F6	8.21	382	698	5.7	17.1	6.72	91.6	19.1	<DL	143.4	109.7	40.5	47.2	0.23	0.14	18.7	17.4	<DL	63.72	0.02	1.03	0.12	35.9	1.30	0.35	0	10	10	0.00	3.4
L1	9.76	331	508	6.5	16.7	6.65	65.8	18.9	0.16	109.8	109.5	2.3	39.7	0.07	0.24	4.8	11.5	<DL	47.52	<DL	0.77	0.08	2.0	0.99	1.73	360	6	367	60.0	12.6
L2	9.64	326	520	5.7	16.1	6.57	64.9	18.8	0.02	109.8	104.0	0.9	38.4	0.05	0.22	<DL	12.9	<DL	47.19	0.02	0.93	0.10	2.7	0.89	1.75	284	13	297	21.9	14.0
L3	9.66	320	509	6.5	16.4	6.67	65.6	19.1	<DL	106.8	103.1	<DL	37.1	0.06	0.21	<DL	10.5	<DL	48.02	<DL	1.25	0.10	3.8	1.02	1.80	337	21	358	16.1	10.1
L4	9.56	317	518	5.9	16.7	6.65	65.7	18.7	0.04	106.8	102.7	<DL	37.0	0.07	0.22	<DL	10.4	<DL	47.25	0.01	0.79	0.14	23.6	0.962	1.69	405	3	408	135.0	16.4
GW1	7.52	435	575	9.9	9.3	1.85	54.5	12.0	<DL	94.6	93.3	85.8	20.1	0.04	0.22	<DL	17.2	<DL	36.10	0.01	0.54	<DL	32.0	0.91	0.63	89	45	134	2.0	2.5
GW2	7.70	393	655	9.9	13.8	0.94	99.4	18.3	<DL	112.9	96.8	94.5	36.4	0.13	0.27	4.4	27.3	<DL	61.51	0.02	0.87	0.08	126.6	0.23	0.22	20	51	72	0.4	1.8
GW3	6.83	398	670	11.0	20.6	2.63	85.3	17.5	<DL	161.7	90.6	44.2	41.5	0.17	0.19	<DL	856.8	<DL	93.74	0.05	1.37	<DL	19.9	0.53	0.45	316	103	419	3.1	4.0
GW4	6.76	395	616	11.8	16.6	3.05	86.4	13.6	<DL	106.8	100.7	72.9	26.4	0.20	0.67	15.4	8.2	<DL	32.34	0.02	1.03	0.16	6.5	2.38	1.85	604	537	1 141	1.1	2.1
GW5	6.85	281	575	10.1	15.0	2.93	92.4	15.7	0.04	201.4	69.1	3.9	44.9	0.14	0.27	<DL	1949.0	<DL	86.76	0.04	1.16	0.35	86.2	1.48	0.36	69	83	152	0.8	2.6
SP1	7.14	445	665	7.5	17.0	5.57	105.7	19.7	<DL	122.0	127.2	62.3	46.4	0.67	0.20	8.0	1156.0	<DL	105.10	0.27	1.56	0.09	416.9	1.60	3.14	18	131	149	0.1	ND
SP2	6.93	35	617	7.7	15.4	5.49	102.2	17.5	6.27	347.8	60.0	5.2	40.4	1.29	0.29	1 579.0	35 250.0	<DL	343.70	0.19	1.79	0.26	5.4	2.60	5.52	61	21	83	2.9	ND
SP3	6.86	39	623	7.8	16.0	4.97	98.8	16.4	7.45	338.7	49.8	4.6	38.7	1.33	0.28	1 485.0	28 865.0	<DL	329.64	0.21	1.83	0.29	6.7	2.41	4.89	54	14	68	3.9	ND
SP4	7.31	484	868	7.6	16.9	3.48	126.0	13.6	0.11	146.4	114.0	136.7	54.9	0.61	0.17	<DL	5.3	<DL	83.44	0.02	0.94	0.25	2.7	0.95	0.39	16	33	49	0.5	ND
SP7	8.44	94	487	8.1	15.9	6.22	58.9	16.3	0.44	97.6	110.5	<DL	39.1	0.47	0.27	89.2	27.3	42.0	58.74	<DL	0.90	0.18	4.5	0.98	1.89	235	65	300	3.6	ND

DL = detection limit, ND = not determined.

4. Results

4.1. Geochemistry and mineralogy of soils

The results of the geochemical analysis of the samples in the studied profile are summarized in Table 2 and Fig. 2. The redox potentials in the profiles indicate highly oxidizing conditions except for profile M3, in which there is a substantial decrease in the redox potential below the groundwater level. The soils are usually neutral and are acidic only in the surface layer, probably caused by the presence of organic acids. The distribution of total As is highly variable. In the M1 profile, the highest As concentration is at the base of the profile (5690 mg kg^{-1}), in the M2 profile this is in its centre (1600 mg kg^{-1}) and in the M3 profile this is just below the groundwater level (4080 mg kg^{-1}). The total $S^{-2,0}$ is always below the detection limit of 10 mg kg^{-1} and the SO_3 content is elevated only in the surface soil layer, caused by atmospheric deposition and/or by the combination of capillary rise and high evaporation in the surface. The total As in all the profiles exhibits a medium correlation with the total Fe ($r=0.73$, $p=0.0002$, $n=21$); changes in the correlations between the individual profiles are minimal with a deviation up to 5%. The oxalate-extractable Fe fraction of the total Fe content in the soil increases smoothly in the M2 profile and above the groundwater level of M3 profile towards the surface (Fig. 2E) and corresponds to up to 17.6% in the M3 profile. The As and Fe contents in this extraction are not correlated ($r=0.39$, $p=0.08$, $n=21$), similar to the As extraction and the extractions of Mn and Al; nonetheless, the bonding of As to poorly crystalline oxyhydroxides is significant, as the oxalate-extractable As fraction of the total soil As corresponds to 8.1–79.9%. There is a marked increase in the As content bonded in this way, ranging from 28.2 to 79.9% in the surface soil layer, especially above the groundwater level of profile M3 (Fig. 2E). Water-soluble As constitutes a maximum of 0.57% of the total As. Its distribution in profiles M1 and M2 is not correlated with the total amount of As, while this correlation is high in profile M3 below the groundwater level ($r=0.91$, $p=0.03$, $n=5$). It thus follows that the concentration of water-soluble As is controlled by the total As content only below the groundwater level. Water-soluble As(III) predominates over As(V) in profile M1 and below the groundwater level of profile M3, where the As(III)/As(V) ratio is inversely proportional to the water soluble NO_3 (Fig. 3B). Conversely, As(V) predominates in profile M2 and above the groundwater level in M3.

Through a combination of XRD and EMPA measurements, the presence of Ba pharmacosiderite [$Ba_{(1-n)}$,Ca_n)($Fe_{4-m}Al_m$)(AsO_4)$_3$(OH)$_5\cdot 5H_2O$], arseniosiderite, scorodite and As-bearing Fe oxyhydroxides, specifically goethite and hematite [Fe_2O_3] were determined in the heavy-mineral fraction of the soil (Fig. 4). Whereas the diffraction peaks of arsenate minerals are relatively narrow, those of goethite are usually broad, suggesting lower crystallinity, especially in the surface soil horizons of M1 and M3. In addition, XRD in all the samples from the M1 soil profile and partially in the samples close to the groundwater level in the M3 profile exhibits two very broad peaks at 35° and 63° 2θ, which can be attributed to ferrihydrite. These findings are in accordance with the results of oxalate extraction, which yielded the highest levels of oxalate-extractable Fe in the M1 profile and above the groundwater level of the M3 profile (Fig. 2D). The chemical composition of the minerals is variable (Fig. 5, Table 3) and frequently differs from the ideal structural formula, with the exception of scorodite. Barium pharmacosiderite often contains an elevated amount of Ca (maximally 5.0 wt.%) at the expense of Ba, and also a slightly elevated Al content (maximum of 3.3 wt.%) at the expense of Fe. The lowest content of Ca has been detected in the rare cubic crystals of Ba pharmacosiderite (Fig. 6A). Arseniosiderite often replaces pharmacosiderite (Fig. 6B) or forms discrete leaf-like aggregates (Fig. 6D). Iron oxyhydroxides contain up to 16.0 wt.% As and frequently also have elevated Ca contents (maximally 3.0 wt.%). Arsenic and Ca-rich Fe oxyhydroxides are always associated with arseniosiderite, with which they form intimate intergrowths or mutually replace one another (Fig. 6C). The distribution of As minerals is variable in the soil profiles and is mostly related to the variations in the total As content (Fig. 2C). Point counting of selected grains from the heavy-mineral samples shows that As minerals form up to 0.64 wt.% in the 0.125–0.25 mm grain-size fraction (Fig. 4). The distribution of the individual As-bearing mineral phases in the profiles also differs, and two general trends can be seen in the studied fraction (Fig. 4): (i) there is an elevated content of ferrihydrite and goethite at the expense of

Table 2
Selected physico-chemical characteristics of the soil and sediment samples.

Site	Depth (cm)	pH	Eh (mV)	Total metal, arsenic and sulphur species						Oxalate-extractable metal, arsenic and sulphur				
				Al_2O_3 (wt.%)	SO_3 (g/kg)	$S^{-2,0}$ (g/kg)	Fe (g/kg)	As (mg/kg)	Ba (mg/kg)	Fe-ox (mg/kg)	Al-ox (mg/kg)	S-ox (mg/kg)	As-ox (mg/kg)	Ba-ox (mg/kg)
M1	0–34	5.85	546	21.5	<DL	<DL	67.8	2920	395	1892	905	29	237	38
	34–53	6.33	550	20.1	<DL	<DL	48.3	1820	460	1589	596	18	322	36
	53–100	6.97	491	20.8	<DL	<DL	58.7	2490	364	2369	513	16	645	49
	100–125	7.18	513	19.4	0.72	<DL	41.2	1340	520	2004	435	16	618	41
	125–181	7.04	496	21.0	<DL	<DL	59.2	1800	278	1897	370	15	559	38
	181–224	6.93	493	18.9	<DL	<DL	66.7	5690	640	3863	320	18	1950	63
M2	0–40	5.98	478	20.0	0.49	<DL	33.5	710	660	2398	1233	29	131	36
	40–60	6.85	541	21.2	<DL	<DL	48.4	1590	660	1999	678	12	228	50
	60–90	7.25	534	20.8	<DL	<DL	48.5	1600	590	2360	590	12	416	47
	90–116	7.02	523	20.4	<DL	<DL	50.5	1220	500	1707	422	13	318	38
	116–133	6.98	548	20.3	<DL	<DL	50.8	1180	540	1484	359	10	272	20
M3	0–32	6.15	499	17.7	1.08	<DL	29.1	1170	490	5130	1272	94	912	37
	32–52	5.10	451	16.0	<DL	<DL	20.7	283	480	3387	693	15	146	17
	52–74	6.65	450	19.8	<DL	<DL	36.1	630	470	4475	741	13	264	25
	74–95	6.67	426	20.3	<DL	<DL	50.3	2090	393	2863	791	11	719	27
	95–115	6.61	436	20.1	<DL	<DL	42.0	1770	480	1779	668	11	499	22
	115–165	6.89	412	21.2	<DL	<DL	50.6	4080	790	1821	650	6	669	67
	165–198	6.88	341	20.4	<DL	<DL	53.7	3330	750	1564	353	10	602	73
	198–245	6.97	334	20.1	<DL	<DL	53.3	2340	530	1764	320	10	389	37
	245–292	7.19	307	20.1	<DL	<DL	46.6	1970	490	1389	340	10	405	23
	292–351	7.51	297	19.9	<DL	<DL	50.6	2310	520	1429	254	8	446	16
S1	5	7.14	445	17.9	<DL	<DL	29.2	1154	645	2784	449	37	470	66
S2	5	6.93	35	17.4	<DL	3.29	37.6	1193	725	9375	1223	929	590	64
S4	5	7.31	484	17.5	<DL	<DL	22.9	139	511	1639	238	19	67	20
S7	5	8.44	94	16.0	<DL	1.43	13.3	58	484	2769	282	310	29	41

DL = detection limit.

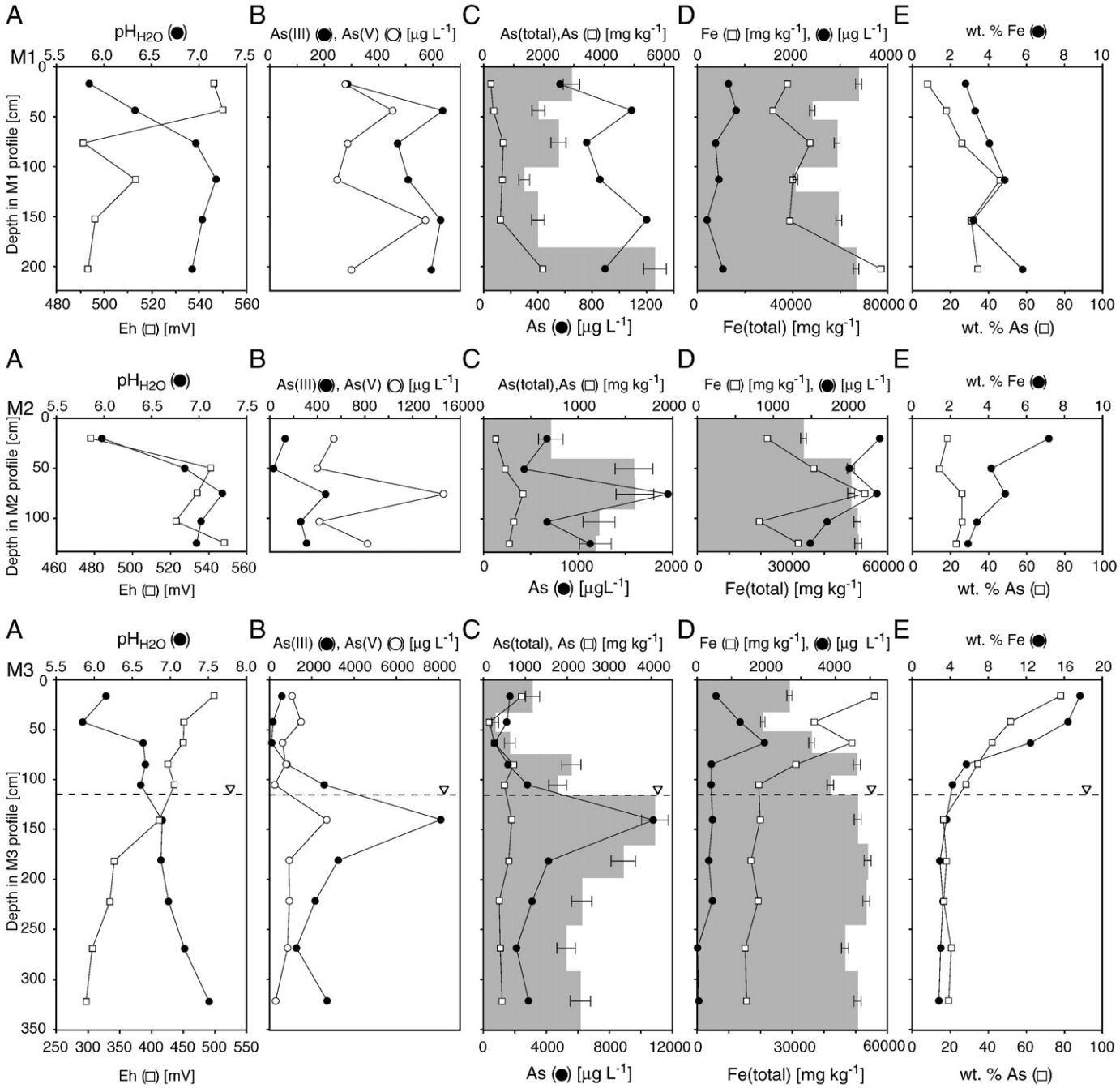

Fig. 2. Depth variations in the distribution of the physico-chemical parameters in the soil profiles: (A) pH (black circle) and Eh (open square); (B) concentrations of water-soluble As(III) (black circle) and As(V) (open circle); (C) water-soluble (black circle), oxalate-extractable (open square), and total As concentrations (grey field); (D) water-soluble (black circle), oxalate-extractable (open square), and total Fe concentrations (grey field); (E) fractions of As (open square) and Fe (black circle) of the total soil As and Fe (measured by XRF), respectively bound to oxalate extractions. Water-soluble concentrations are given in µg L^{-1}; oxalate-extractable concentrations are given in mg kg^{-1}; the total contents are given in mg kg^{-1}.

arsenate minerals in the highest parts of the soil profiles and (ii) the amount of arseniosiderite increases upwards in the soil profile at the expense of pharmacosiderite. The latter finding is supported by the total Ba content (Fig. 3A), which indicates the largest amount of Ba pharmacosiderite below the groundwater level.

4.2. Geochemistry and mineralogy of sediments

The physico-chemical parameters of the sediments are characterised in Table 2. The stream sediments are almost neutral, while the fishpond sediments are more basic. The redox potentials of sandy samples S1 and S4 are oxidative and those of clay-muddy samples S2, and S7 are reducing, caused mainly by the high organic matter content. The total As in the sediments reflects the distance of the sampling site from the primary deposit; samples S1 and S2 are characterized by more than 1100 mg kg^{-1} As, while sample S4 situated 500 m downstream contains 139 mg kg^{-1} As. The total As in the fishpond bottom sediments is much lower (58 mg kg^{-1}), probably as a result of the occasional dredging of the bottom sediments. A high $S^{-2,0}$ content was found in reducing samples S2 and S7; conversely, the $S^{-2,0}$ and SO_3 contents were below the detection limit in the oxidizing samples S1 and S4. The As bonding to poorly crystalline Fe oxyhydroxides seems obvious from the oxalate extractions and corresponds to between 41 and 49% of the total As content. The As concentration in

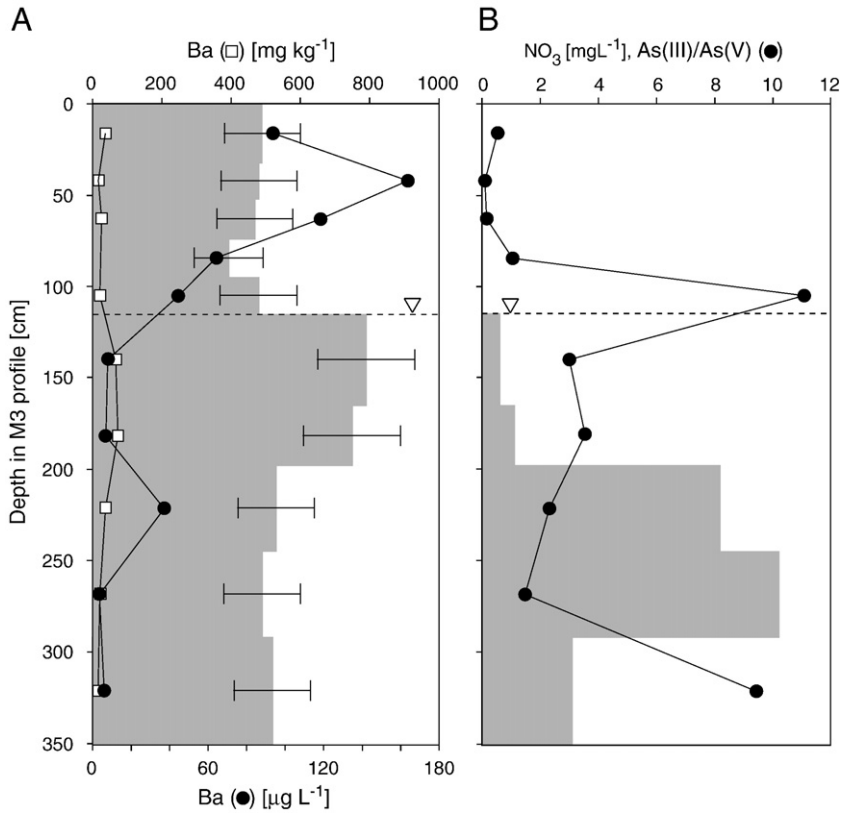

Fig. 3. (A) Total content of Ba (grey area) [mg kg^{-1}] in soil profile M3 and its concentration in the water-soluble (black circle) [µg L^{-1}] and oxalate-extractable fractions (open square) [mg kg^{-1}]. (B) Concentration of water-soluble NO_3 fraction (grey area) and the ratio of water-soluble As(III)/As(V) (black circle) in the M3 profile. The concentration of NO_3 above the groundwater level is below the detection limit (DL = 0.3 mg L^{-1}).

the pore waters is not correlated with the total As in the solid phase or with the As extractable in the oxalate. While the concentration of pore-water As is always lower than that in the related surface water, the concentrations of the other elements are usually similar. Considerable differences were found only between the chemistry of the pore-water of SP2, SP3 and related surface water sample F2 (Table 1), which is manifested in elevated concentrations of bicarbonate, in the high NH_4/NO_3 ratio and in the low sulphate concentration in the pore water.

The XRD results in the heavy-mineral fractions of sediments indicate the presence of goethite and hematite (Fig. 4) with the exception of the most reducing sample S2, where Fe oxyhydroxides were not detected. Goethite completely predominates over hematite in stream samples S1 and S4, and their contents are roughly equal in the fishpond bottom sediment, S7 (Fig. 4). In addition to crystalline Fe phases, a broad diffusive peak in sample S4 may indicate the presence of ferrihydrite. A high As content (up to 9.3 wt.%) and the related Ca (up to 1.7 wt.%) concentration were confirmed in some of these Fe oxyhydroxides by EMPA, similar to their contents in Fe oxyhydroxides in soils. However, most Fe oxyhydroxides in the sediments contain substantially smaller amounts of As than Fe oxyhydroxides in the soil samples (Table 3), usually around 1 wt.%. EMPA also very rarely indicated the presence of pharmacosiderite minerals, arseniosiderite and clay minerals, containing max. 1.3 wt.% As.

4.3. Water chemistry

The analyses of the water samples are presented in Table 1. All the waters are close to neutral pH or are slightly alkaline. The major element chemistry was dominated by Ca (54.5–114.2 mg L^{-1}) and HCO_3 (94.6–201.4 mg L^{-1}). Intense agricultural activity in this area has probably resulted in NO_3 concentrations in water that often exceed the drinking water standards (>50 mg L^{-1}). The concentrations of Fe, Mn and Al were very low, with Mn generally exceeding Fe (Table 1).

The As concentration decreases from 449 µg L^{-1} (F1) to 32 µg L^{-1} (F5) in the direction downstream from the MWD ore mineralization after the confluence with the Čelina stream, whose As concentration (F6) represents the reference background value for stream water in the area. Arsenic(V) predominates in sample F1, which has highly oxidizing character, while As(III) predominates in other stream samples with a lower redox potential. The highest As(III)/As(V) ratio was found in sample F3, which was taken under the fishpond in the muddy area with a high organic matter content. Arsenic(III) then predominated until the confluence with the Čelina stream, in which As(III) was not detected. The As concentration in the fishpond varied from 297 to 408 µg L^{-1} with a striking predominance of As(III) (As(III)/As(V) > 16). Higher As concentrations in the groundwater were found in deeper wells GW3 ~ 1.9 m and GW4 ~ 5.6 m, with values of 419 and of 1141 µg L^{-1}, respectively, in the close vicinity of the village, which were used as drinking water supplies in the past. Lower As concentrations (72–152 µg L^{-1}) were found in shallow reclaiming wells of subsurface drainage (GW1, GW2 and GW5), whose depth never exceeded 0.6 m. Similar to the total dissolved As concentration, the distributions of As(III) and As(V) are also variable and the As(III)/As(V) ratio attains values from 0.3 to 2.0. Arsenic(III) generally predominates in deeper wells, but its distribution is best related to the DOC concentration, as there is a high correlation between As(III)/As(V) and DOC ($r = 0.90$, $p = 0.038$, $n = 5$) in groundwater. Analogously, a high correlation ($r = 0.82$, $p < 0.001$, $n = 15$) between As(III)/As(V) and DOC was recorded for all MWD water samples.

4.4. Speciation calculations

Table 4 gives the results of the PHREEQC thermodynamic modelling for selected water samples. The measured redox potential is usually

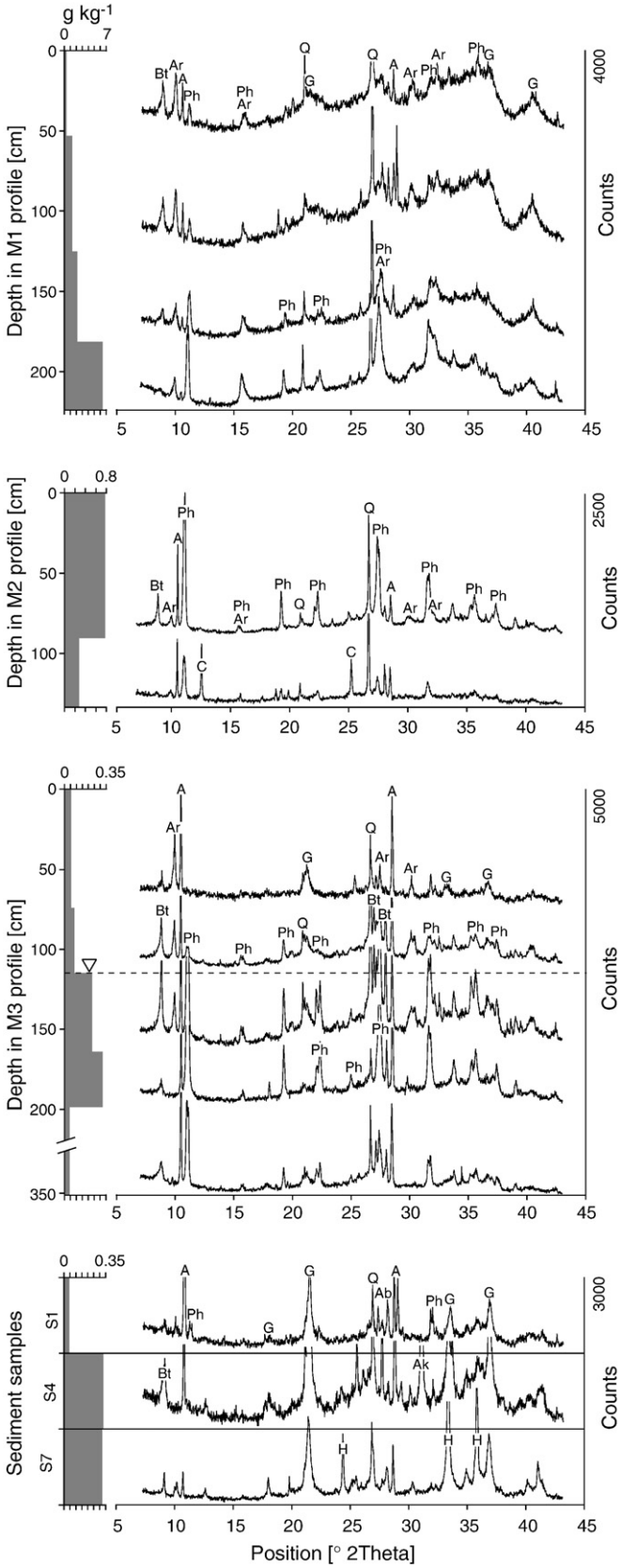

Fig. 4. XRD powder patterns from the heavy-minerals of the 0.25–0.125 mm fraction in soil profiles M1–M3 and stream (S1 and S4) and fishpond sediments (S7). Abbreviations and corresponding PDF reference code of As-bearing minerals: Ar: Arseniosiderite (00-013-0134); G: Goethite (00-029-0713); H: Hematite (01-089-0599); Ph: Ba pharmacosiderite (00-034-0154). Abbreviations of other minerals: A: amphibole, Ab: albite, Ak: ankerite, Bt: biotite, C: chlorite and Q: quartz. The weighted fractions of the separated minerals in the bulk samples are given on the left (grey area).

much higher than the potential calculated from the As(III)/As(V) pair and differs nonsystematically from the potential calculated from the $NH_4(-III)/NO_3(V)$ pair.

Thermodynamic calculations have shown that As(V) occurs in the form of $HAsO_4^{2-}$ (33.3–98.9%), less as $H_2AsO_4^-$ (0.2–66.7%) and only occasionally as AsO_4^{3-} (maximum 1.3%). Arsenic(III) is mostly stable in the form of $H_3AsO_3^0$ (24.8–99.7%) and $H_2AsO_3^-$ (up to 68.2%) can predominate only in the alkaline waters of the fishpond. Under the subsurface conditions, calcite is generally slightly undersaturated ($-1.1<SI<0.0$), while it is usually saturated on the surface ($-0.3<SI<1.9$). The waters are mostly highly supersaturated with respect to crystalline Fe oxyhydroxides, specifically goethite ($SI>6.4$) and hematite ($SI>14.8$). Under oxidizing conditions, ferrihydrite is also highly supersaturated ($SI>3.8$), while it is undersaturated in the reducing environment of the stream sediment S2 ($SI<-0.9$). Arsenate minerals (scorodite, Ca arsenate) are always highly undersaturated in all the samples (Table 4). The reducing environment of the SP2 and SP3 pore waters is far from saturation with respect to Fe(II) sulphides and As(III) sulphides ($SI<-27$).

5. Discussion

5.1. Arsenic in the solid phase — implications for As mobility

Arsenopyrite was found very rarely as a relict replaced by secondary arsenates and Fe oxyhydroxides in a mineralized saprolite near the M1 profile (Filippi et al., 2004). The preservation of arsenopyrite under oxidizing conditions was a result of a protective layer of secondary minerals, which reduced the rate of oxidation of sulphidic S and As in the arsenopyrite (Walker et al., 2006). In the pH range from 4 to 10, the decomposition of arsenopyrite follows Eq. (1):

$$FeAsS + 7H_2O \leftrightarrow Fe^{2+}(aq) + H_3AsO_3(aq) + 11H^+ + 11e^- + SO_4^{2-} \quad (1)$$

The exact speciation of As(III) depends on the pH; nonetheless, H_3AsO_3 is stable in a broad range of groundwater pH values ($pK_a = 9.23$; Nordstrom and Archer, 2003).

Arsenic(III) and Fe(II) are oxidized in accordance with Eqs. (2)–(4) (the products of the reactions are a result of the thermodynamic speciation of the groundwater; see Table 4).

$$H_3AsO_3 + H_2O \leftrightarrow HAsO_4^{2-} + 4H^+ + 2e^- \quad (2)$$

$$H_3AsO_3 + H_2O \leftrightarrow H_2AsO_4^- + 3H^+ + 2e^- \quad (3)$$

$$Fe^{2+} + 3H_2O \leftrightarrow Fe(OH)_3(aq) + 3H^+ + e^- \quad (4)$$

Scorodite, the minerals of the pharmacosiderite group and arseniosiderite are formed under oxidizing conditions with high activity of dissolved As(V) (Sadiq, 1997; Magalhães, 2002). These conditions probably occurred at MWD mainly in the oxidizing zone of saprolite with arsenopyrite. Because of the low filtration coefficient of the saprolite (10^{-7}–10^{-10} m s^{-1} according to Morávek, 1991), a high concentration gradient of dissolved As(V) can occur in the immediate vicinity of the weathered arsenopyrite. Under the initial conditions of oxidation of arsenopyrite, where the pH of the solution decreases to below 3 because of the oxidation of dissolved Fe(II) (Eq.(4)) and As(III) (Eqs.(2), (3)), scorodite is formed according to Eq. (5) (Krause and Ettel, 1989):

$$H_2AsO_4^- + Fe^{3+} + 2H_2O \rightarrow FeAsO_4 \cdot 2H_2O(s) + 2H^+ \quad (5)$$

The released acidity is neutralised by the dissolution of calcite and aluminosilicates (Drahota and Pertold, 2005), which release cations

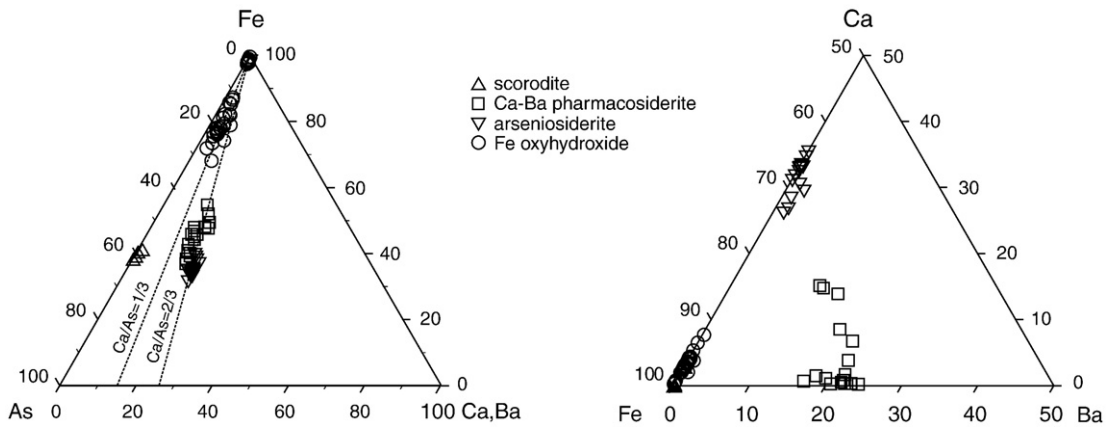

Fig. 5. Ternary diagram of the composition of secondary arsenates and Fe oxyhydroxides in soil profiles and sediments. The dashed lines with numbers are the Ca/As molar ratios. Mineral identifications are based on electron microprobe analysis.

into the solution and increase its alkalinity. At an increased activity of the basic cations, Ba pharmacosiderite can be formed (Eq. (6)).

$$3H_2AsO_4^- + (1-n)Ba^{2+} + nCa^{2+} + 4Fe(OH)_3(aq) \leftrightarrow (Ba_{(1-n)}, Ca_n)Fe_4(AsO_4)_3(OH)_5 \cdot 5H_2O + H_2O + OH^- \quad (6)$$

It follows from Eq. (6) that precipitation of Ba pharmacosiderite can also buffer the acidity of the solution from which it is formed. The chemical variability of pharmacosiderite, which, in MWD, represents a solid solution close to the Ba and K end members (Filippi et al., 2007) with variable Ca content (Fig. 5), can be explained by various compositions of the solutions from which it was formed, or by later ion exchange with the solutions (Mutter et al., 1984; Morin et al., 2002). Despite the arguments supporting the crystallization of pharmacosiderite during soil formation (Filippi et al., 2007), our data do not exclude hydrothermal origin of pharmacosiderite. Small cubic crystals of Ba pharmacosiderite may indicate that they originated from a late hydrothermal event involving the reaction of barite and arsenopyrite. The latter hypothesis is supported by the lack of barite in the soil, representing the major source of Ba for weathering solutions, and similar genetic interpretation of the pharmacosiderite origin in the literature (e.g., Walenta, 1994; Morin et al., 2002). Arseniosiderite has a higher Ca/Fe molar ratio (i.e. 2/3) than Ca pharmacosiderite with Ca in the mineral structure (molar ratio 1/3) and it is thus probable that it was formed in a solution with very high Ca ion activity (Swash and Monhemius, 1995). The Ca source in the solution mostly corresponds to dissolution of calcite, which buffers the pH of the solution at about 6–8 (Table 1) and thus the formation of arseniosiderite can be assumed to occur at a much higher pH than that for the pharmacosiderite group of minerals. Arseniosiderite can be formed by direct precipitation from solution (Eq. (7)).

$$3H_2AsO_4^- + 2Ca^{2+} + 3Fe^{3+}(OH)_3(aq) \leftrightarrow Ca_2Fe_3(AsO_4)_3O_2 \cdot 3H_2O + 4H_2O + H^+ \quad (7)$$

However, in association with pharmacosiderite or scorodite, it always forms younger massive aggregates and veins, which evidently replace Ba pharmacosiderite (Fig. 6B). Similar findings have been described by Filippi et al. (2007) in MWD soils and by Paktunc et al. (2003, 2004) in the Ketza River mine tailing. Pharmacosiderite minerals thus probably incongruently decompose to arseniosiderite according to Eq.(8).

$$(Ba_{(1-n)}, Ca_n)Fe_4(AsO_4)_3(OH)_5 \cdot 5H_2O + (2-n)Ca^{2+} \rightarrow Ca_2Fe_3(AsO_4)_3O_2 \cdot 3H_2O + Fe(OH)_3(aq) + (1-n)Ba^{2+} + 2H_2O + 2H^+ \quad (8)$$

This process leads to an increasing amount of arseniosiderite at the expense of pharmacosiderite minerals towards the surface of the M1 and M3 soil profiles (Fig. 4). This theory is supported by EMPA study, which documented massive replacement of Ba pharmacosiderite by arseniosiderite above the groundwater level of profile M3 (Fig. 6B). The release of Ba during ion exchange or dissolution of Ba pharmacosiderite may be promoted by an increasing amount of water-soluble Ba towards the surface in soil profile M3 (Fig. 3A), whereas the largest amount of Ba pharmacosiderite occurred below the groundwater level.

Iron oxyhydroxides are the most important reservoir of As in the MWD stream sediments and are also common in the studied MWD soils. Under oxidizing conditions, goethite and hematite are thermodynamically most stable (Table 4), although the occurrence of

Table 3
Averaged electron microprobe analyses (EMPA) (wt.%) of Fe(III) oxyhydroxides and arsenate minerals in the heavy fraction (d>2.81) of the soil and sediment samples.

Mineral	SiO_2	Al_2O_3	Fe_2O_3	MnO	K_2O	CaO	BaO	As_2O_5	Total	N
Iron (III) oxyhydroxide										
In soil	2.10	1.39	66.46	0.17	0.01	1.94	0.15	13.23	85.89	31
S.D.	1.15	1.20	8.64	0.24	0.01	1.08	0.40	7.07	4.59	
In sediment	1.68	1.69	66.47	0.25	0.00	1.41	0.01	7.23	80.97	5
S.D.	1.08	1.53	11.03	0.18	0.00	0.89	0.01	6.89	4.01	
Scorodite	0.08	0.40	34.58	0.01	0.06	0.03	0.01	54.80	92.28	4
S.D.	0.13	0.39	0.73	0.01	0.09	0.02	0.02	3.60	1.21	
Pharmacosiderite	0.73	3.15	33.58	0.04	0.57	1.84	7.24	36.91	83.98	20
S.D.	0.72	1.85	3.49	0.04	1.25	2.52	1.65	5.92	5.65	
Arseniosiderite	1.11	0.29	28.48	0.10	0.02	13.30	0.19	40.97	84.85	16
S.D.	0.97	0.20	1.51	0.09	0.02	1.70	0.23	4.85	6.41	

N = number of analyses, S.D. = standard deviation.
The total is given for the whole set of elements analysed, including Na_2O, MgO, P_2O_5 and S, which had contents below 0.12, 0.24, 0.48 and 0.29 wt.%, respectively.

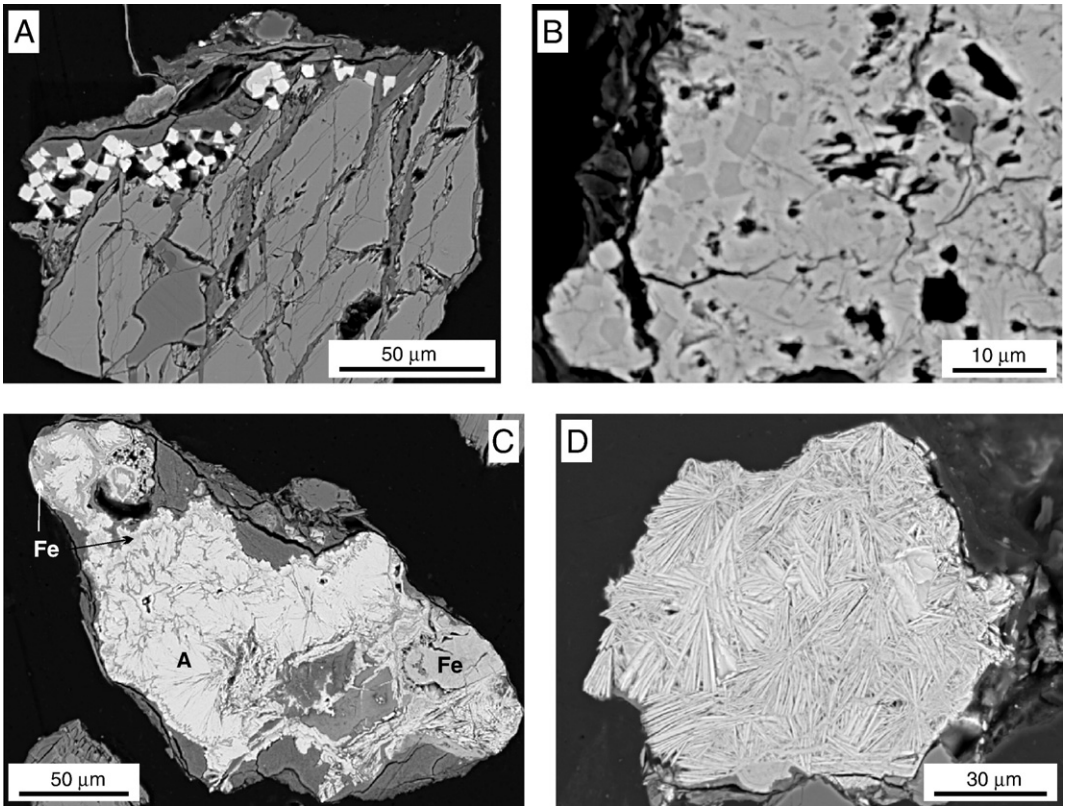

Fig. 6. Backscattered electron micrographs of (A) cubic crystals of Ba pharmacosiderite (soil profile M3: 165–198 cm), (B) cubic crystals of Ba pharmacosiderite (middle grey) surrounded and replaced by the lighter mass of younger arseniosiderite (soil profile M3: 115–165 cm), (C) arseniosiderite (A: white) in equilibrium with As- and Ca-rich Fe oxyhydroxides (Fe: middle grey) (soil profile M2: 125–181 cm), and (D) leaf-like aggregate of arseniosiderite (soil profile M2: 53–100 cm). The mineral identifications are based on electron microprobe analysis.

metastable ferrihydrite has been confirmed in the soil and stream sediments in a mineralogical study (Drahota and Pertold, 2005). Iron oxyhydroxides frequently contain elevated amounts of Ca (on the basis of analysis of 28 grains from all the soil and sediment samples), which are highly correlated with the As ($r=0.82$, $p<0.0001$, $n=36$). The average As/Ca molar ratio of 3.2 means that there are approximately 3.2 arsenate ions for every 1 Ca ion in the Fe oxyhydroxide (Fig. 5). Interpretation of the data suggests several options. The presence of Ca^{2+} could modify the surface charge characteristics of the Fe oxyhydroxide and could thus increase the amount of sorbed As (Smith et al., 2002). However, the close association of the Fe oxyhydroxides with arseniosiderite (e.g., Fig. 6C) tends rather to indicate that Ca- and As-bearing Fe oxyhydroxides could represent amorphous Ca-bearing and As-rich Fe oxyhydroxides (up to 16.0 wt.%

Table 4
Calculated As aqueous species, redox potentials of the As(III)/As(V) and NH_4(−III)/NO_3(V) couples, and the saturation indices (S.I.) for selected samples of the Mokrsko stream (F1, F2), the fishpond (L1), the groundwater (GW2–GW5) and the sediment pore water (SP1–SP7).

pH		F1	F2	L1	GW2	GW4	GW5	SP1	SP2	SP7
		7.65	7.85	9.76	7.70	6.76	6.85	7.14	6.93	8.44
As (V)	(mg L^{-1})	402	75	6	51	537	83	131	21	65
	AsO_4^{3-} (%)	0.0	0.0	1.2	0.0	0.0	0.0	0.0	0.0	0.0
	$HAsO_4^{2-}$ (%)	79.4	75.3	98.6	81.4	33.3	37.9	54.7	42.8	95.8
	$H_2AsO_4^-$ (%)	20.6	24.6	0.2	18.6	66.7	62.1	45.4	57.2	4.2
As(III)	(mg L^{-1})	47	346	360	20	604	69	18	61	235
	$H_2AsO_3^-$ (%)	1.8	1.4	68.2	2.1	0.3	0.3	0.5	0.3	9.9
	$H_3AsO_3^0$ (%)	98.3	98.6	31.8	97.9	99.7	99.7	99.5	99.7	90.1
Eh (mV)	field	462	350	331	393	395	281	445	35	94
	As(III)/As(V)	5	−29	−285	−20	58	57	55	38	−122
	NH4(−III)/NO3(V)	493	–	218	–	–	416	–	401	–
S.I.	Calcite	−0.2	−0.3	1.6	0.0	−1.1	−0.7	−0.6	−0.4	0.5
	Ferrihydrite	3.0	2.9	2.1	2.4	2.4	–	2.5	−0.9	3.3
	Goethite	7.4	7.2	6.4	6.7	6.7	–	6.8	3.4	7.6
	Hematite	16.7	16.3	14.8	15.4	15.3	–	15.5	8.7	17.1
	Scorodite	−5.4	−6.2	−12.3	−7.1	−4.7	–	−5.6	−9.5	−7.5
	Arsenolite	−10.7	−9.0	−9.9	−11.5	−8.6	−10.4	−11.5	−10.5	−9.4
	$Ca_3(AsO_4)_2 \cdot 4H_2O$	−9.2	−10.9	−8.9	−10.6	−11.3	−12.6	−11.3	−13.5	−9.5
	Realgar	−106	−87	−109	−97	−86	−70	−98	−33	−58
	Orpiment	−281	−231	−290	−257	−227	−185	−259	−86	−154
	Mackinawite	−96	−78	−100	−88	−78	–	−89	−27	−49
	Pyrite	−157	−127	−164	−142	−125	–	−143	−39	−78

As) presumably with an arseniosiderite structure or a mixture of As-bearing Fe oxyhydroxide (up to 8 wt.% As) with finely divided arseniosiderite (Paktunc et al., 2003, 2004). In the latter case, it follows from the average As/Ca ratio that Fe oxyhydroxides contain approximately 3.4 mol of adsorbed and/or structurally incorporated As to 3 mol of As in coprecipitated arseniosiderite.

5.2. Controls on As speciation in the waters

5.2.1. Reducing conditions

The flat areas north and west of the village of Mokrsko and in the valley of the Mokrsko stream are characterized by a high groundwater level. In combination with microbially controlled decomposition of organic matter, reducing conditions can be formed in these areas, which we found in several samples close to the surface (samples SP2, SP3, SP7). Under these conditions, the concentration of dissolved As can be controlled by the solubility of the sulphides and will thus be dependent mainly on the rate of the microbial reduction of sulphate. Sulphide minerals may be present in the reducing shallow subsurface of the MWD, as the content of $S^{-2,0}$ in samples S2 and S7 is more than two orders higher than in the other samples of stream sediments in an oxidizing environment (S1 and S4). We assume that these are not preserved sulphides of primary mineralization, but rather newly formed As(III) or Fe(II) sulphides, for several reasons: (i) the sulphate concentration in the reducing pore waters SP2 and SP3 is only half that in the related surface water (F2) (Table 1), probably caused by the precipitation of Fe(II) or As(III) sulphides (e.g., Rittle et al., 1995); (ii) the oxidized stream sediments (e.g., sample S1), which could be a source of solid matter for the reducing S2 and S7 downstream, have $S^{-2,0}$ below the detection limit, and thus do not contain sulphides (sample S1). The equilibrium calculations of the pore waters SP2, SP3 and SP7 from a depth of 5 cm in the sediment indicate high undersaturation with respect to pyrite and Fe(II) monosulphides, as well as to As(III) sulphides (Table 4). However, when the redox potential in the sediment samples decreases to approximately −130 mV and −350 mV, the pore water will be saturated with respect to Fe(II) sulphides and As(III) sulphides, respectively. Oversaturation can be expected in the deeper parts of the sediment, where the physico-chemical characteristics of the pore water are not influenced by mixing with surface stream water, as expected for SP2, SP3 and SP7. It follows from the activity diagram for As(III) vs. Fe(II) vs. pH (Wilkin and Ford, 2006) that the precipitation of As(III) sulphides will be more probable at higher As(III) concentrations, at lower pH or at reduced Fe(II) concentrations. The concentration of dissolved As(III) in the neutral to weakly acidic SP2, SP3 and SP7 is, however, not higher than the solubility of realgar and orpiment (according to O'Day et al., 2004), and thus the most probable mechanism controlling the concentration of dissolved As in the reducing sediments of MWD is adsorption and coprecipitation on the mineral surface of Fe(II) sulphides. This hypothesis is also supported by thermodynamic modelling, which indicates earlier supersaturation with respect to pyrite and mackinawite than for As(III) sulphides during a gradual decrease in the redox potential in the sediment.

5.2.2. Transition redox conditions

A redox transition occurs between the areas in which secondary arsenate minerals and Fe oxyhydroxides are stable and the areas in which Fe(II) or As(III) sulphides are precipitated. In this transition zone, the total dissolved As concentration is controlled by the rate of the dissolution of scorodite, pharmacosiderite, arseniosiderite and As-bearing Fe oxyhydroxides. On the other hand, the concentration of dissolved As will be controlled by the rate of reduction of sulphate which is substantially affected by microbial activity (Kirk et al., 2004). The distribution of dissolved sulphide in the transition zone is usually not sufficient to cause precipitation of As sulphides and so the highest concentration of dissolved As occurs there (e.g., McCreadie et al., 2000; O'Day et al., 2004). This situation was found in soil profile M3, where the increase in the concentration of water-soluble As from 3000 μg L^{-1} at a depth of 292–351 cm, to 10 800 μg L^{-1} at a depth of 115–165 cm (Fig. 2C) indicates that the upper boundary of the transition zone is immediately below the groundwater level, which is located at a depth of 115 cm in M3. Since the water-soluble As closely follows the solid phase As below the groundwater level in soil profile M3, the most likely source of the high concentration of dissolved As is dissolution of arsenate minerals and Fe oxyhydroxides. Reductive dissolution is assumed because these minerals are relatively insoluble. Laboratory experiments with arsenate minerals and Fe oxyhydroxides indicate that dissolution rates are several orders of magnitude greater in the presence of a reductant (e.g., Arnold et al., 1988; Rochette et al., 1998; Cummings et al., 1999). The lower water-soluble As concentrations below 2 m in the M3 soil profile (Fig. 2C) follow the rapid decrease in the amount of As-bearing minerals (Fig. 4), among which only pharmacosiderite occurred in minor to trace quantities always enclosed in aluminosilicates that protected the arsenate from the dissolution. The absence of Fe oxyhydroxides at the depth of soil profile M3 supports the hypothesis of the reductive dissolution, since the equilibrium calculations indicate that the groundwater and even the reducing pore waters are supersaturated with respect to Fe oxyhydroxides (Table 4). Nevertheless, the occurrence of arsenate minerals and Fe oxyhydroxide below the groundwater level, as demonstrated by XRD and EMPA, is in contradiction with the conditions of their origin in an unsaturated environment. The most likely explanation suggests a temporal change in the hydrological condition and/or microbial activity that may play an important role in the current redox state of groundwater and dissolution of As-bearing minerals in the transition zone. The impact of the reduction on the redox-sensitive arsenate minerals and Fe oxyhydroxides at MWD has been roughly estimated by the sequential extraction of MWD soil (Filippi et al., 2007), which confirmed that 50–80% of the As is bonded to a certain degree to the reducible fraction of Fe oxyhydroxides and arsenate minerals (NH_4-oxalate/ascorbic acid according to Wenzel et al., 2001), while bonding of As to the soluble, strongly adsorbed and residual fractions is less important.

Dissolved As(III) predominates in the M1 profile and below the groundwater level of profile M3, although it is not thermodynamically stable under these conditions. It can thus be concluded that the microbial reduction of As(V) is faster than abiotic or biotic oxidation of As(III). On the other hand, NO_3 could be an important oxidant of As(III) and Fe(II) under anoxic conditions (Weber et al., 2001; Senn and Hemond, 2002). Although no direct evidence is available for the oxidation of As(III) by NO_3 at MWD, it seems from the negative correlation of NO_3 and the As(III)/As(V) ratio in profile M3 (Fig. 3B) that this process may control As speciation under the anoxic conditions of MWD. A similar relationship could hold in the fishpond (L1–L4) with a high As(III) concentration and negligible NO_3 concentration (Table 1).

5.2.3. Oxidizing condition

Under the oxidizing conditions at MWD, the concentration of dissolved As seems to be controlled by the rate of oxidation of arsenopyrite, the solubility of scorodite, pharmacosiderite and arseniosiderite and, on the other hand, by the degree of adsorption of As oxyanions, particularly on the surface of Fe oxyhydroxides. Swash and Monhemius (1995) found, in the Ca–Fe–AsO_4 system, that an increase in the Ca content in the phase leads to increased solubility and that the opposite trend holds for the Fe content. It follows from the study of the solubility of scorodite, pharmacosiderite and arseniosiderite that pharmacosiderite has the lowest solubility (0.223 mg L^{-1} at pH 6.6) and arseniosiderite has the highest solubility, which gradually decreases from 28 mg L^{-1} (pH 8.1) to 6.7 mg L^{-1} (pH 6.85) (Krause and Ettel, 1989). However, arseniosiderite generally predominates over pharmacosiderite minerals in the highly oxidizing environment of soil profiles M1 and M3, which means that arseniosiderite is highly stable under the given conditions, although it is undersaturated in all the

waters studied, according to the solubility values (Krause and Ettel, 1989). The increased stability of arseniosiderite is probably caused by an ion effect in which the high activity of the Ca^{2+} reduces the solubility of arseniosiderite. Swash and Monhemius (1995) and Juillot et al. (1999) described a similar reduction in the solubility of Ca arsenates through the addition of limestone to the system. In addition to their high solubilities, Ca arsenates can also slowly and incongruently dissolve to calcite at elevated CO_2 partial pressures and simultaneously release As (V) into solution (Robins, 1981). Frau and Ardau (2004) assume the decomposition of arseniosiderite in the Baccu Locci stream sediments (Sardinia, Italy) in this way; see Eq. (9) at pH>7.

$$Ca_2Fe_3(AsO_4)_3O_2 \cdot 3H_2O + 2CO_2 + 6H_2O \leftrightarrow 3HAsO_4^{2-} + 2CaCO_3 + 3Fe(OH)_3 + 6H^+ \quad (9)$$

Nonetheless, Nishimura et al. (1983) assumed that this reaction will be effective only at pH>8.3. Juillot et al. (1999) do not assume the decomposition of Ca arsenates through this reaction in weakly acidic media with high CO_2 partial pressure. Consequently, carbonation of arseniosiderite (Eq. (9)) or Ca pharmacosiderite is not likely to occur at the atmospheric pressure of CO_2, as the pH of the oxidizing environments at MWD is almost neutral and diagenetic calcite has not been found in the solids.

As discussed above, As is probably bonded in coprecipitated Ca–Fe arsenate in Fe oxyhydroxides (Paktunc et al., 2004) and a comparable amount of As is adsorbed and/or incorporated in the structure of Fe oxyhydroxide. Thus, some As can readily be released by the dissolution of coprecipitated Ca–Fe arsenate, while adsorbed As and incorporated As in the structure remain relatively stable under the oxidizing conditions. Adsorbed As also retards the transformation of the poorly crystalline forms of Fe oxyhydroxides (presumably ferrihydrite at MWD) to the more stable goethite and hematite (Waychunas et al., 1993). The content of Fe oxyhydroxides is usually the highest under the surface conditions of the soil profiles (M1 and M3), caused by their stability and precipitation of the released Fe(III) from arsenates (Eq. (8) and Eqs. (5) and (7) in the opposite direction) and some aluminosilicates, such as biotite and amphibole. As a consequence, the Fe oxyhydroxides would presumably be the main carrier of As in the surface parts of the soil profiles (Fig. 2E) and in the oxidizing stream sediments.

The As concentration in the surface waters is highly correlated with aqueous Sb ($r = 0.94$, $p < 0.0001$, $n = 10$), which occurs only at very low concentrations from 0.35 to 2.13 μg L^{-1} (Table 1). Antimony is bonded in Au accessory minerals in the MWD and can be present in up to 0.35 wt.% in arsenopyrite (J. Zachariáš, personal communication). In the dissolved state, it forms particularly the SbO_3^- anion which, similar to As, is very readily adsorbed on Fe oxyhydroxides (Scheinost et al., 2006). The correlation of As and Sb in surface waters thus indicates that their concentrations are controlled by the same processes, particularly adsorption/desorption reactions on Fe oxyhydroxides.

The adsorption of As can be affected by the occurrence of other competitive ions in the system, which can directly compete for the available binding sites and indirectly influence the adsorption through changes in the electrostatic charge at the solid surface. The low concentrations of phosphate common in soils affected by agricultural activities were not found to affect the mobility of As in soil samples from the MWD (Sisr et al., 2007); the effect of sulphates and other anions can be completely neglected, as they are not present in sufficient amounts to affect the adsorption of As (Jain and Loeppert, 2000; Smith et al., 2002).

6. Conclusions

Arsenic speciation and mobility in the MWD were studied by a series of complementary mineralogical and geochemical methods. The data obtained show that natural As contamination of soils and waters is substantially affected by a set of (bio)geochemical processes, which determine the consequent mobility and speciation of As under various redox conditions in the solid-water system. These processes are described by the schematic model in Fig. 7.

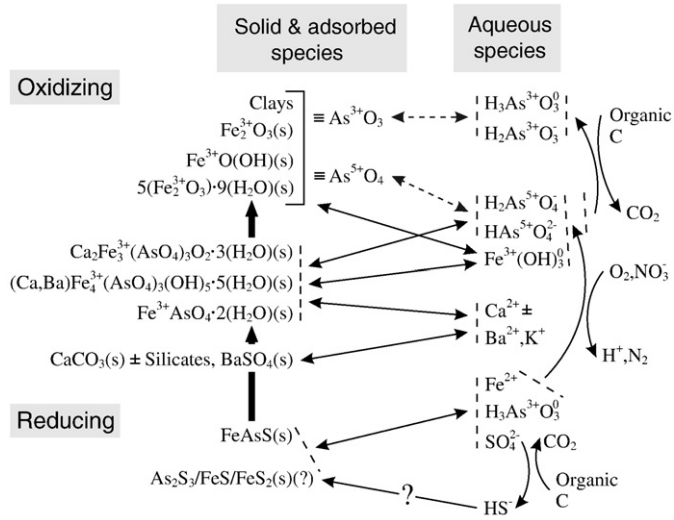

Fig. 7. Biogeochemical model of As under oxidizing and reduction conditions, summarizing the main precipitation/dissolution and adsorption/desorption reactions controlling the mobility of As at the Mokrsko-West deposit. The full arrows denote precipitation/dissolution reactions, the dashed arrows denote adsorption/desorption reactions and the curved arrows denote oxidation/reduction reactions, which can be catalyzed by microbiological activity (oxidation of organic matter, denitrification reactions). The names of the minerals that are characterized by their chemical compositions are given in the Sections 2 and 4.1.

The highest concentrations of dissolved As in the MWD occur in the redox transition zone, where As is most likely released by reductive dissolution of scorodite, pharmacosiderite, arseniosiderite and As-bearing Fe oxyhydroxides. The dissolution is probably related to the spatial and/or temporal variations of the redox state in this zone due to groundwater level elevation and/or variations in the microbial activity, which is indicated by the positive correlation of DOC with high As(III)/As(V) ratios in waters (Perdue and Ritchie, 2003). In surface waters, the As(III)/As(V) ratios are the highest at muddy sites rich in organic matter. It is thus probable that organic substances are the most important electron donor in the dissimilatory processes in the MWD. The further fate of the dissolved As species depends on where it is transported and on the (bio)chemical conditions in the particular environment. Under reducing conditions with high microbial activity, it is probably bonded to newly formed sulphides. Reduced As(III) is evidently released from anoxic soils below the groundwater level and from stream sediments in the hyporheic zone into the oxidizing surface waters, and is oxidised to thermodynamically stable As(V). Consequently, there are high concentrations of dissolved As(III) under the oxidizing conditions in the Mokrsko stream which, however, gradually decrease downstream as As(III) is oxidized and As is sequestered in the solid stream sediments.

Acknowledgements

This work was supported by GA UK No. 339/2004/B GEO, GA ČR 205/06/0298, Ministry of Education (MSM 0021620855), and project of the Geological Institute of the Czech Academy of Science AVOZ30130516. We wish to thank V. Sedláček and V. Böhmová (both from the Service Laboratory of Physical Methods, Institute of Geology AS ČR) for their assistance with heavy-mineral separation and the EMPA study, respectively. Z. Górecká (Central Laboratory of the Czech Geological Survey, Prague) is thanked for overnight anion analyses and S. Randáková (Institute of Chemical Technology, Prague) for XRF analyses. M. Štulíková and K. Štulík are also thanked for improving the English of the manuscript.

References

Arnold RG, Dichristina TJ, Hoffmann MR. Reductive dissolution of Fe(III) oxides by *Pseudomonas* sp. 200. Biotechnol Bioeng 1988;32:1081–96.

Ball JW, Nordstrom DK. User's manual for WATEQ4F with revised thermodynamic data base and test cases for calculating speciation of major, trace, and redox elements in natural waters. US Geol Surv Open-File Rep; 1991. p. 91–183.

Bowell RJ, Morley NH, Din VK. Arsenic speciation in soil porewaters from the Ashanti Mine, Ghana. Appl Geochem 1994;9:15–22.

Cherry JA, Shaikh AU, Tallman DE, Nicholson RV. Arsenic species as an indicator of redox conditions in groundwater. J Hydrol 1979;43:373–92.

Cullen WR, Reimer KJ. Arsenic speciation in the environment. Chem Rev 1989;89: 713–64.

Cummings DE, Caccavo F, Fendorf S, Rosenzweig RF. Arsenic mobilization by the dissimilatory Fe(III)-reducing bacterium *Shewanella alga* BrY. Environ Sci Technol 1999;33:723–9.

Dedina J, Tsalev DL. Hydride Generation Atomic Absorption Spectrometry. Chichester: John Wiley&Sons; 1995. p. 526.

Dove PM, Rimstidt JD. The solubility and stability of scorodite $FeAsO_4.2H_2O$. Am Miner 1985;70:838–44.

Drahota P, Pertold Z. Weathering of As-rich rocks in the Celina–Mokrsko gold district, Bohemian Massif (CZ). In: Öhlander B, editor. Securing the Future 2005, vol. 1. International Conference on Mining and the Environment, Skellefteå, Sweden; 2005. p. 242–51.

Drahota P, Pačes T, Pertold Z, Mihaljevič M, Skřivan P. Weathering and erosion fluxes of arsenic in watershed mass budgets. Sci Total Environ 2006;372:306–16.

FAO. World Reference Base for Soil Resources: World Soil Resources Report. Rome: FAO; 1998. p. 88. No. 84.

Fernández P, Sommer I, Cram S, Rosas I, Gutiérrez M. The influence of water-soluble As (III) and As(V) on dehydrogenase activity in soils affected by mine tailings. Sci Total Environ 2005;348:231–43.

Filippi M, Doušová B, Machovič V. Mineralogical speciation of arsenic in soils above the Mokrsko–west gold deposit, Czech Republic. Geoderma 2007;139:154–70.

Filippi M, Goliáš V, Pertold Z. Arsenic in contaminated soils and anthropogenic deposits at the Mokrsko, Roudný, and Kašperské Hory gold deposits, Bohemian Massif (CZ). Environ Geol 2004;45:716–30.

Frau F, Ardau C. Mineralogical controls on arsenic mobility in the Baccu Locci stream catchment (Sardinia, Italy) affected by past mining. Mineral Mag 2004;68:15–30.

ICDD. JCPDS PDF-2 database. Newton Square, PA, USA: ICDD; 2002.

Jain A, Loeppert RH. Effect of competing anions on the adsorption of arsenate and arsenite by ferrihydrite. J Environ Qual 2000;29:1422–30.

Janatka J, Morávek P. Geochemical exploration in the Jílové belt: case history of the Celina deposit, Bohemian Massif, Czechoslovakia. J Geochem Explor 1990;37: 367–84.

Jílek V. Mokrsko-geomedical study. Technical Report, Geofond. Prague; 1985. (in Czech).

Juillot F, Ildefonse Ph, Morin G, Calas G, De Kersabiec AM, Benedetti M. Remobilization of arsenic from buried wastes at an industrial site: mineralogical and geochemical control. Appl Geochem 1999;14:1031–48.

Keon NE, Swartz CH, Brabander DJ, Harvey C, Hemond HF. Validation of an arsenic sequential method for evaluating mobility in sediments. Environ Sci Technol 2001;35: 2778–84.

Kirk MF, Holm TR, Park J, Jin Q, Sanford RA, Fouke BW, et al. Bacterial sulfate reduction limits natural arsenic contamination in groundwater. Geology 2004;32:953–6.

Krause E, Ettel VA. Solubilities and stabilities of ferric arsenate compounds. Hydrometallurgy 1989;22:311–37.

Langmuir D, Mahoney J, Rowson J. Solubility products of amorphous ferric arsenate and crystalline scorodite ($FeAsO_4{\cdot}2H_2O$) and their application to arsenic behavior in buried mine tailings. Geochim Cosmochim Acta 2006;70:2942–56.

Macur RE, Jackson CR, Botero LM, McDermott TR, Inskeep WP. Bacterial populations associated with the oxidation and reduction of arsenic in an unsaturated soil. Environ Sci Technol 2004;38:104–11.

Macur RE, Wheeler JT, McDermott TR, Inskeep WP. Microbial populations associated with the reduction and enhanced mobilization of arsenic in mine tailings. Environ Sci Technol 2001;35:3676–82.

Magalhães MCF. Arsenic. An environmental problem limited by solubility. Pure Appl Chem 2002;74:1843–50.

Malec J. Research study on gold and accompanying minerals at the Mokrsko deposit. Technical report, Ústav nerostných surovin, Kutná Hora; 1990. (in Czech).

McCreadie H, Blowes DW, Ptacek CJ, Jambor JL. Influence of reduction reactions and solid-phase composition on porewater concentrations of arsenic. Environ Sci Technol 2000;34:3159–66.

Montperrus M, Bohari Y, Bueno M, Astruc A, Astruc M. Comparison of extraction procedures for arsenic speciation in environmental solid reference materials by high-performance liquid chromatography-hydride generation-atomic fluorescence spectroscopy. Appl Organomet Chem 2002;16:347–54.

Morávek P. Čelina — Psí Hory: Au ores, the stage of prospecting. Technical Report, Prague, Czech Republic, Geofond; 1991. (In Czech).

Morávek P, Janatka P, Pertoldová J, Straka J, Ďurišová J, Pudilová M. Mokrsko gold deposit — the largest gold deposit in the Bohemian Massif, Czechoslovakia. Econ Geol Monogr 1989;6:252–9.

Morin G, Calas G. Arsenic in soils, mine tailings and former industrial sites. Elements 2006;2:97–101.

Morin G, Lecocq D, Juillot F, Calas H, Ildefonse Ph, Belin S, et al. EXAFS evidence of sorbed arsenic(V) and pharmacosiderite in a soil overlying the Echassières geochemical anomally, Allier, France. Bull Soc géol France 2002;173:281–91.

Mutter G, Eysel W, Greis O, Schmetzer K. Crystal chemistry of natural and ion-exchanged pharmacosiderites. Neues Jb Miner Monat 1984;4:183–92.

Nishimura T, Tozawa K, Robins RG. The calcium–arsenic–water system. Proceedings MMIJ/Aus. IMM Joint Symposium, Paper JD-2-1, Sendai, Japan; 1983. p. 105–20.

Nordstrom DK, Archer DG. Arsenic thermodynamic data and environmental geochemistry. In: Welch AH, Stollenwerk KG, editors. Arsenic in Ground Water. Boston: Kluwer Academic Publisher; 2003. p. 1–26.

O'Day PA, Vlassopoulos D, Root R, Rivera N. The influence of sulfur and iron on dissolved arsenic concentrations in the shallow subsurface under changing redox conditions. P Natl Acad Sci USA 2004;101:13703–8.

Paktunc D, Foster A, Heald S, Laflamme H. Speciation and characterization of arsenic in gold ores and cyanidation tailings using X-ray absorption spectroscopy. Geochim Cosmochim Acta 2004;68:969–83.

Paktunc D, Foster A, Laflamme G. Speciation and characterization of arsenic in Ketza River mine tailings using X-ray absorption spectroscopy. Environ Sci Technol 2003;37:2067–74.

Pansu M, Gautheyrou J. Handbook of Soil Analysis—Mineralogical, Organic and Inorganic Methods. Springer; 2006. p. 993.

Parkhurst DL, Appelo CAJ. User's guide to PHREEQC (Version 2) — a computer program for speciation, batch-reaction, one-dimensional transport, and inverse geochemical calculations. US Geol Surv Water Resour Investig Rep; 1999. p. 99–4259.

Perdue EM, Ritchie JD. Dissolved organic matter in freshwaters. In: Drever JI, Holland HD, Turekian KK, editors. Surface and Ground Water, Weathering, and Soils, vol. 5. Oxford: Elsevier–Pergamon; 2003. p. 273–319.

Puls RW, Paul CJ. Low-flow purging and sampling of ground-water monitoring wells with dedicated systems. Ground Water Monit Remediat 1995;15:116–23.

Rittle KA, Drever JI, Colberg PJS. Precipitation of arsenic during bacterial sulfate reduction. Geomicrobiol J 1995;13:1–11.

Robins RG. The solubility of metal arsenates. Metall Trans B 1981;12:103–9.

Rochette EA, Li GC, Fendorf SE. Stability of arsenate minerals in soil under biotically generated reducing conditions. Soil Sci Soc Am J 1998;65:1530–7.

Sadiq M. Arsenic chemistry in soils: an overview of thermodynamic predictions and field observations. Water Air Soil Pollut 1997;93:117–36.

Scheinost AC, Rossberg A, Vantelon D, Xifra I, Kretzschmar R, Leuz AK, et al. Quantitative antimony speciation in shooting-range soils by EXAFS spectroscopy. Geochim Cosmochim Acta 2006;70:3299–312.

Senn DB, Hemond HF. Nitrate controls on iron and arsenic in an urban lake. Science 2002;296:2373–6.

Sisr L, Mihaljevič M, Ettler V, Strnad L, Šebek O. Effect of application of phosphate and organic manure-based fertilizers on arsenic transformation in soil columns. Environ Monit Assess 2007;135:465–73.

Smith E, Naidu R, Alston AM. Chemistry of inorganic arsenic in soils: II. Effect of phosphorus, sodium, and calcium on arsenic sorption. J Environ Qual 2002;31:557–63.

Sohrin Y, Matsui M, Kawashima M, Hojo M, Hasegawa H. Arsenic biogeochemistry affected by eutrophication in Lake Biwa, Japan. Environ Sci Technol 1997;31:2712–20.

Swash PM, Monhemius AJ. Synthesis, characterization and solubility testing of solids in the Ca–Fe–AsO_4 system. In: Ilynes TP, Blanchette MC, editors. Mining and the Environment, Sudbury '95 CANMET, Ottawa, Canada; 1995. p. 17–28.

UNIQUANT 4. Software for standardless X-Ray Fluorescence Analysis, Omega Data System bv, The Netherlands; 1995.

Voight DE, Brantley SL, Hennet RJC. Chemical fixation of arsenic in contaminated soils. Appl Geochem 1996;11:633–43.

Walenta K. About a barium-pharmacosiderite. Aufschluss 1994;45:73–81. (in German).

Walker FP, Schreiber ME, Rimstidt JD. Kinetics of arsenopyrite oxidative dissolution by oxygen. Geochim Cosmochim Acta 2006;70:1668–76.

Waychunas GA, Rea BA, Fuller CC, Davis JA. Surface chemistry of ferrihydrite: Part 1. EXAFS studies of the geometry of coprecipitated and adsorbed arsenate. Geochim Cosmochim Acta 1993;57:2251–69.

Weber KA, Picardal FW, Roden EE. Microbially catalyzed nitrate-dependent oxidation of biogenic solid-phase Fe(II) compounds. Environ Sci Technol 2001;35:1644–50.

Wenzel WW, Kirchbaumer N, Prohaska T, Stingeder G, Lombi E, Adriano DC. Arsenic fractination in soils using an improved sequential extraction procedure. Anal Chim Acta 2001;436:309–23.

Wilkin RT, Ford RG. Arsenic solid-phase partitioning in reducing sediments of a contaminated wetland. Chem Geol 2006;228:156–74.